Journal of Power Sources 239 (2013) 111–121

Contents lists available at SciVerse ScienceDirect

Journal of Power Sources

journal homepage: www.elsevier.com/locate/jpowsour

Enhanced performance of a novel gel polymer electrolyte by dual plasticizers

Xiang Zuo [a], Xiao-Min Liu [a,*], Feng Cai [a], Hui Yang [a,*], Xiao-Dong Shen [a], Gao Liu [b]

[a] College of Materials Science and Engineering, Nanjing University of Technology, 5 Xinmofan Road, Nanjing, Jiangsu 210009, PR China
[b] Environmental Energy Technologies Division, Lawrence Berkeley National Laboratory, 1 Cyclotron Rd., Berkeley, CA, USA

HIGHLIGHTS

- Polyethylene glycol dilaurate is adopted as the physical cross-linking agent in GPE.
- The GPE exhibits good mechanical property and a relatively high ionic conductivity.
- A cell Li/GPE/$LiFePO_4$ shows discharge capacity 152 mAh/g at 0.1 C at 30 °C.

GRAPHICAL ABSTRACT

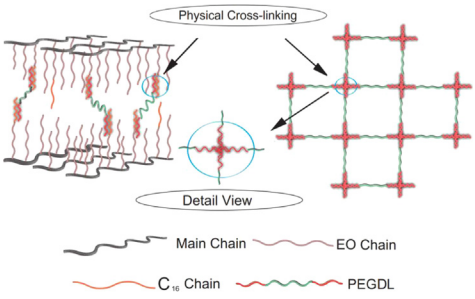

ARTICLE INFO

Article history:
Received 11 October 2012
Received in revised form
25 March 2013
Accepted 25 March 2013
Available online 4 April 2013

Keywords:
Gel polymer electrolyte
Polyethylene glycol dimethyl ether
Methacrylate
Lithium polymer cell

ABSTRACT

In this contribution, polyethylene glycol dilaurate (PEGDL) is synthesized and adopted as the physical cross-linking agent to enhance the performance, especially the mechanical property of the gel polymer electrolytes (GPEs). With polyethylene glycol dimethyl ether (PEGDME) as the main plasticizer and PEGDL as the secondary plasticizer, several gel polymer electrolytes based on a copolymer of methoxy-poly(ethylene glycol) methacrylate (MPEGM) and hexadecal-poly(ethylene glycol) methacrylate (HPEGM) are prepared by UV radiation curing. The relationship between the composition of the GPE and the physical properties, e.g., thermal property, mechanical property and ionic conductivity, is investigated. The lithium ion transference number, lithium/GPE interfacial property and charge–discharge performance of the lithium polymer cell based on the physically cross-linked GPE are studied. The gel polymer electrolyte prepared with the optimum composition exhibits excellent mechanical properties and a relatively high ionic conductivity (8.2×10^{-4} S cm^{-1} at 30 °C). A coin cell Li/GPE/$LiFePO_4$, shows a discharge capacity 152 mAh g^{-1} and 163 mAh g^{-1} when cycled at 30 °C and 50 °C, respectively, under a current density of 0.1 C.

1. Introduction

Polymer electrolytes in lithium ion batteries have attracted much attention recently due to the fabrication flexibility in shape and size for roll-up displays and wearable electronic devices, etc. [1,2], as well as the improvement of reliability and safety to replace the liquid electrolytes. The area of solid polymer electrolytes has gone through various developmental stages. First proposed by Wright [3], polyethylene oxide (PEO) and its derivatives as polymer matrixes could dissolve salts and allow ion transport in amorphous phase [4–6]. However, the linear PEO of high molecular weight tends to crystallize below 65 °C [7], and therefore exhibits fairly low ionic conductivity (10^{-8}–10^{-7} S cm^{-1}). In order to suppress the crystallization, Oligo-(ethylene oxide) is grafted to different polymer backbones, such as polyphospazene [8], polysiloxane [9,10],

* Corresponding authors.
E-mail addresses: lxm3799@yahoo.com (X.-M. Liu), yanghui@njut.edu.cn (H. Yang).

0378-7753/$ – see front matter © 2013 Elsevier B.V. All rights reserved.
http://dx.doi.org/10.1016/j.jpowsour.2013.03.144

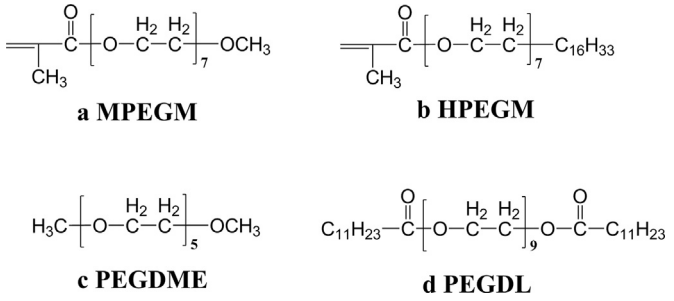

Fig. 1. Chemical structures of MPEGM, HPEGM, PEGDME and PEGDL.

and polymethacrylate [11,12]. Even though the solid polymer electrolytes (SPEs) show good mechanical property and chemical stability, they still suffer from poor ion conductivity about 10^{-5}–10^{-4} S cm^{-1}, which is far from the practical application level. By incorporating organic solvents (plasticizer) into SPEs, gel polymer electrolytes are developed to increase the ion conductivity [13]. Recently, oligomeric poly(ethylene glycol) dimethyl ether (PEGDME) is used as the plasticizer to enhance the ionic conductivity and the safety of polymer electrolyte because of its high donor number and high flash point [14]. The addition of PEGDME into the polymer electrolyte decreases the glass transition temperature (T_g) of the EO chains, enhances segmental motion, and improves ionic conductivity, but promotes deterioration of the electrolyte's mechanical property. Chemical cross-linking has been widely adopted to improve the mechanical stability of the GPEs while ensuring the good conductivity at room temperature. At present the conductivity of the chemical cross-linked gel electrolytes is about 2.1×10^{-4}–7.8×10^{-4} S cm^{-1} [15–20].

An alternative way to prepare gel polymer electrolyte is to make use of aggregating or self-assembling polymer architectures which consist of two chemically dissimilar polymer segments [21,22]. At low temperatures or in the absence of solvent, an electrostatic repulsion between the polymer segments induces their local segregation, or "micro-phase separation", into periodically spaced nanoscale domains. In this way, physically cross-linked networks are formed. With methoxy-poly(ethylene glycol) methacrylate [MPEGM, Fig. 1a] and hexadecyl-poly(ethylene glycol) methacrylate [HPEGM, Fig. 1b], a novel polymer matrix, poly(MPEGM-co-HPEGM) [PMH, Fig. 2a], was synthesized in our previous study [23]. It has been found that C_{16} chains from HPEGM may expand the space and weaken the interaction among main chains and side chains by distributing in the polymer randomly and disrupting the regular arrangement of EO chains. Therefore the ionic conductivity can be raised through the improvement in the flexibility of the main chains and the mobility of the EO chains provided that the content of HPEGM is low in the polymer. For example, PMH25 (copolymerized from 75 wt% MPEGM and 25 wt% HPEGM) exhibits a relatively high conductivity (1.3×10^{-4} S cm^{-1} at 30 °C). Hence, PMH could be a good candidate for the polymer matrix of GPEs by introducing nonvolatile polyethylene glycol dimethyl ether [PEGDME, Fig. 1c] as the ion conducting plasticizer. Our initial results show that PMH copolymerized from less than 30 wt% HPEGM can host more than 50 wt% PEGDME, thus the resulting GPE exhibits a relatively high conductivity (1.2×10^{-3} S cm^{-1} at 30 °C) but very poor mechanical stability. When the content of HPEGM is more than 30 wt% in PMH, the GPE presents good mechanical stability properly due to the formation of the physically cross-linked matrix by the aggregation of C_{16} as shown in Fig. 2b. However, the limited swelling of the polymer network can host at most 50 wt% PEGDME without leakage, resulting in relatively low conductivity of the obtained GPEs ($\sim 4 \times 10^{-4}$ S cm^{-1} at 30 °C). In order to obtain a PMH-based GPE with both sufficient mechanical stability and high conductivity, a polyethylene glycol derivative, polyethylene glycol dilaurate [PEGDL, Fig. 1d], is synthesized and incorporated into the GPE. With long hydrocarbon chains (C_{11}) on both ends, PEGDL may form physical cross-linking with either C_{16} chains [Fig. 2c] or itself [Fig. 2d], which may improve the mechanical property of the obtained GPE.

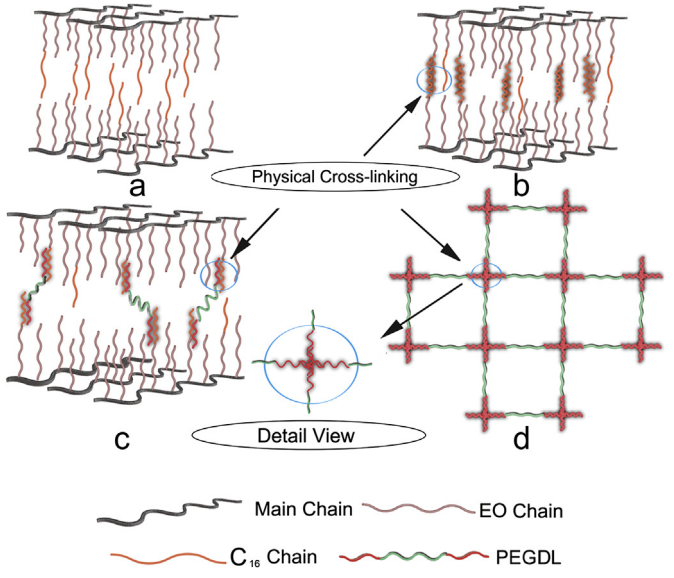

Fig. 2. Schematic illustrations for the ideal structure of: PMH with low content of HPEGM (a); PMH with high content of HPEGM (b); physically cross-linked network formed by PMH and PEGDL (c); physically cross-linked network formed by PEGDL itself (d).

In this work, PEGDME and PEGDL as the plasticizer are used to prepare the PMH-based gel electrolytes. The mechanical property of the GPEs with PEGDME is first discussed in detail. Then the GPEs with PEGDME/PEGDL at various ratios are compared to the GPEs with PEGDME only. Since the ratio of the monomers, the amounts of the plasticizers may affect the properties of GPEs, the relationship between the composition of the gel electrolyte and the physical properties, i.e., thermal property, mechanical property, and ionic conductivity, is explored to guide the preparation of the GPE with good properties. Then the lithium ion transference number, lithium/GPE interfacial property and charge–discharge performance of the lithium polymer cell based on physically cross-linked GPE are studied.

2. Experiment

2.1. Synthesis of macro-monomers

Two macro-monomers, MPEGM and HPEGM, were prepared by using methacryloyl chloride (98%, Alfa Aesar) to esterificate the terminal hydroxyl groups of methoxy-poly(ethylene glycol) (M_w = 350, Alfa Aesar) and hexadecyl-poly(ethylene glycol) (M_w = 534, TCI), respectively. A well stirred mixture of 0.10 mol methoxy-poly(ethylene glycol) [or hexadecyl-poly(ethylene glycol)] and 0.12 mol triethylamine in 250 mL dry dichloromethane (DCM) was maintained in an ice-water bath. Methacryloyl chloride (0.12 mol) was added dropwise to the above mixture. After 12-h stirring, followed by filtration, vacuum evaporation, and column chromatography purification, the macro-monomers were obtained.

2.2. Synthesis of polyethylene glycol dilaurate (PEGDL)

Polyethylene glycol dilaurate was prepared by using lauric acid (Alfa Aesar) to esterificate the terminal hydroxyl groups of poly (ethylene glycol) (M_w = 400, Aladdin). A total of 0.10 mol

poly(ethylene glycol) and 0.25 mol lauric acid were added into about 5–7 g *p*-toluenesulfonic acid and 100 mL toluene in a flask. After about 5-h reflux at 130 °C, the residual toluene in the mixture was removed by reduced pressure distillation. The resulting solution was poured into 500 mL DCM. After cooled down, washed by lithium hydroxide solution and deionized water successively for three times, dried by anhydrous magnesium sulfate, and filtration, the oily product was further purified by vacuum evaporation to remove the solvent.

2.3. Pretreatment of PEGDME

Since the trace amount of residual hydroxyl groups in commercial PEGDME may increase the interfacial resistance between lithium electrode and electrolyte, the residual hydroxyl groups should be eliminated before PEGDME was employed as the plasticizer. A solution of 0.50 mol PEGDME (Alfa Aesar) in 500 mL dry DCM was maintained at 0 °C. Certain amount of sodium hydride was added slowly into the solution, followed by 3-h stirring to ensure sodium hydride and hydroxyl to react completely. After filtration to remove sodium hydride and the side product of sodium alcohol, the obtained solution was washed by 150 mL 0.10 mol L^{-1} HCl. Then PEGDME was obtained by fractional distillation of the collected non-aqueous layer at reduced pressure. After dried under dynamic vacuum overnight, the treated PEGDME was stored over activated molecular sieves for more than 24 h in an Ar-circulating glove box before use.

2.4. Preparation of electrolytes

MPEGM, HPEGM, PEGDL, PEGDME and $LiClO_4$ (99.9%, Aladdin) at a certain ratio were mixed to prepare a homogeneous viscous solution. The mixture was stirred for 3 h in an Ar-filled glove box and then poured on a Teflon plate. After small amount of photo-initiator (2,2-dimethoxy-2-phenylacetophenone, 0.5 wt% of monomers) was added, the solution was solidified by photo-induced radical polymerization under UV irradiation. Then heterogeneous solid as white and translucent thin membrane was obtained, which is attributed to the polymerization-induced phase separation mechanism [19,24,25]. The similar approach was adopted to prepare GPE without PEGDL while PMH30 and PEGDME were at the weight ratio of 30:70.

2.5. Physical property

Thermal analysis was conducted with a DSC200F3 (NETZSCH) differential scanning calorimeter over the temperature range of −100 to 100 °C under N_2 atmosphere at the scan rate of 10 °C min^{-1}. The sample, placed in the aluminum container, was first heated to 100 °C, then cooled down to −100 °C and scanned. Thermogravimetric analysis (TGA) was conducted under nitrogen environment at the heating rate of 10 °C min^{-1} from 25 °C to 500 °C by a TA instrument STA409PC (NETZSCH).

The morphology of GPE films was measured by NIKON LV100POL microscope equipped with a CCD camera. The mechanical strength of films was determined from stress–strain measurement using a Shimadzu AGS-X tensile testing machine at the rate of 5 mm min^{-1}.

2.6. Electrochemical property

The ionic conductivity of the samples was measured by alternating current (AC) impedance spectroscopy using an impedance analyzer (PARSTAT2273) in the frequency range of 0.1 Hz to 10^6 Hz. The polymer electrolyte was sandwiched by two polished stainless-steel electrodes, sealed in a testing cell within an Argon-housed dry box. Then the testing cell was measured in the temperature range from 10 °C to 80 °C.

The lithium ion transference number (t_+) of the electrolyte was measured according to the Evans and Abraham method [26] by applying 50 mV polarization to the cell, calculated by the following equation:

$$t_+ = \frac{I_s(\Delta V - I_0 R_{i,0})}{I_0(\Delta V - I_s R_{i,s})} \quad (1)$$

By taking into account the resistance change in the polymer electrolyte, Eq. (1) can be rewritten as Eq. (2) [27],

$$t_+ = \frac{I_s R_{b,s}(\Delta V - I_0 R_{i,0})}{I_0 R_{b,0}(\Delta V - I_s R_{i,s})} \quad (2)$$

where ΔV is the potential applied across the cell, I_0 and I_s are the initial and steady-state dc current, $R_{b,0}$ and $R_{b,s}$ are the initial and final resistance of the electrolyte, and R_0 and R_s are the initial and steady-state resistance of the passivating layer.

The electrochemical stability of the electrolyte was determined by cyclic voltammetry (CV) using Pt as the working electrode and Li as the counter and reference electrode. The scan was performed at the scan rate of 5 mV s^{-1} from −0.5 V to 6.0 V vs. Li^+/Li at 30 °C. The interfacial resistance between electrolyte and electrodes (lithium disk with 16 mm diameter) was analyzed by AC impedance spectroscopy using PARSTAT 2273 impedance analyzer for a Li/GPE/Li cell.

The coin-type (CR2032) lithium polymer cell was prepared using the physically cross-linked GPE film, $LiFePO_4$ (Changsha Yunchou Power Technology, China) and metalic lithium as electrolyte, cathode and anode, respectively. A N-methyl pyrrolidone (NMP)-based slurry composed of a mixture of $LiFePO_4$ (90 wt%), PVDF binder (5 wt%) and acetylene carbon black (5 wt%) is prepared. Then the cathode electrode is fabricated by coating the slurry on an aluminum foil. A roll press is carried out on the dried electrode in order to enhance the particulate contact and adhesion to the Al foil. The active mass loading corresponds to a capacity of about 2.5 mAh cm^{-2}. The assembled cells are initially subjected to two formation cycles at a constant current of 0.05 C at 30 °C using a BT-2000 battery testing system (Arbin, USA) in the voltage range of 2.5–4.2 V vs. Li^+/Li. After formation cycles, the discharge–charge tests were carried out under various C-rate at both 30 °C and 50 °C.

3. Results and discussion

3.1. GPE electrolytes with PEGDME

Table 1 summarizes the appearance and the ionic conductivity (σ) of several gel electrolytes based on PMH and PEGDME when [Li]:[EO] is 1:20. It can be seen that PMH copolymerized from less than 30 wt% HPEGM can host more than 50 wt% PEGDME, hence the resulting GPEs exhibit relatively high conductivity. For example, the sample electrolyte with the composition of 30 wt% PMH20 and 70 wt% PEGDME presents the conductivity of 1.2×10^{-3} S cm^{-1} at 30 °C, which meets the practical cell application requirement. However, the poor mechanical strength of these films as described in Table 1 makes them difficult to assemble the cell. On the other hand, the GPEs made from PMH with more than 30 wt% HPEGM are elastic and can be fabricated to mechanical stable thin films (<200 μm). The reason for good mechanical strength of GPEs with more than 30 wt% HPEGM may be related to the more content of the physical cross-linking formed between the adjacent C_{16} chains.

Table 1
The appearance characteristic and ionic conductivity of polymer electrolytes based on PMH with different PEGDME contents when [Li]:[EO] = 1:20.

Polymer matrix	PEGDME content (wt%)	Appearance	σ (S cm^{-1}) at 30 °C
PMH20	0	Very stiff and brittle[a]	8.4×10^{-5}
	50	Stiff and brittle[b]	6.8×10^{-4}
	60	Very brittle[c]	8.2×10^{-4}
	70	Very brittle[c]	1.2×10^{-3}
PMH30	0	Stiff and brittle[a]	7.6×10^{-5}
	50	Waxy and brittle[b]	5.7×10^{-4}
	60	Very brittle[c]	7.6×10^{-4}
	70	Very brittle[c]	1.1×10^{-3}
PMH40	0	Tough[a]	2.1×10^{-5}
	50	Elastic[b]	4.9×10^{-4}
	60	*	–
	70	*	–
PMH50	0	Highly tough[a]	1.5×10^{-5}
	50	Elastic[b]	4.1×10^{-4}
	60	*	–
	70	*	–

* Plasticizer leakage.
[a] Solid polymer electrolytes.
[b] Relatively dimensionally stable electrolyte which can be stripped from the mold when the thickness is less than 200 μm.
[c] Poor mechanical property of the electrolyte which cannot be stripped from the mold when the thickness is less than 200 μm.

However, excess physical cross-linking confines the swelling of the polymer network, which limits the incorporation of PEGDME, thus leading to a relatively low conductivity of the obtained GPEs ($\sim 4 \times 10^{-4}$ S cm^{-1} at 30 °C).

3.2. GPE electrolytes with PEGDME and PEGDL

In order to obtain a PMH-based GPE with both sufficient mechanical strength and high conductivity, polyethylene glycol dilaurate (PEGDL) is synthesized and incorporated into the GPE. PEGDL has long hydrocarbon chains (C_{11}) on two ends. Physical cross-linking may be formed among PEGDL and C_{16} chains of HPEGM, which may improve the mechanical property of the obtained GPE.

Fig. 3a (Fig. 3b) displays the effect of the GPE composition on the mechanical performance of the GPE composed of PMH20 (PMH30), PEGDL and PEGDME. The three arrows represent the electrolyte composition at the weight percentage. Table 2 summarizes the composition, conductivity and T_g of GPEs which can form elastic films. The GPE films made from PMH20 (PMH30), PEGDME and PEGDL are elastic. In contrast, the GPE films made from PMH20 (PMH30), PEGDME without PEGDL are fragile as list in Table 1. When the weight percentage of PMH20 (PMH30) is kept constant, the addition of PEGDL results in a slight decrease of the conductivity. On the other hand, when the weight percentage of PEGDME is constant, the addition of PEGDL improves the conductivity due to the reduction of the weight ratio of PMH. In this study, the GPE with the highest conductivity, 8.2×10^{-4} S cm^{-1} at 30 °C, has the composition of 30 wt% PMH30, 10 wt% PEGDL and 60 wt% PEGDME at [Li]:[EO] = 1:20.

The effect of PEGDL on the mechanical property of the GPE films can be directly visualized in Fig. 4. The viscous solution of 30 wt% PMH30 and 70 wt% PEGDME is pictured in Fig. 4(a-1), and the resulting GPE film is pictured in Fig. 4(a-2). The results of preliminary bending test and tensile test are shown in Fig. 4(a-3) and Fig. 4(a-4), respectively. The viscous solution of 30 wt% PMH30, 60 wt% PEGDME and 10 wt% PEGDL is pictured in Fig. 4(b-1), and the resulting white and translucent thin membrane is shown in Fig. 4(b-2). The results of preliminary bending test and tensile test are shown in Fig. 4(b-3) and Fig. 4(b-4), respectively. The results indicate that the addition of PEGDL does improve the mechanical property of the GPE film, which may be attributed to the increased cross-link density and the micro-phase separation. In order to examine the micro-phase separation, the micrographs of the above two GPE films are taken with an optical microscope. Only homogeneous shade is observed in the film without PEGDL (Fig. 4(a-5)). In contrast, remarkable sea islands are observed in the film with PEGDL (Fig. 4(b-5)), indicating the presence of the two-phase structure, which is common in micro-phase separation systems [25,28]. Here the micro-phase separation may be caused by the immiscibility between the polar EO chains complexed with lithium salt and non-polar long hydrocarbon chains. The different transmittances of EO and hydrocarbon phases cause the appearance of bright and shade domains. By calculating the content of each component, it can be concluded that the bright and shade domains represent the hydrocarbon chains and EO chains complexed with lithium salt, respectively.

3.3. Effect of lithium salt concentration

The dependence of the ionic conductivity and the glass transition temperature (T_g) of GPEs on the lithium salt concentration expressed as the ratio of [Li]:[EO] is plotted in Fig. 5, where the GPE

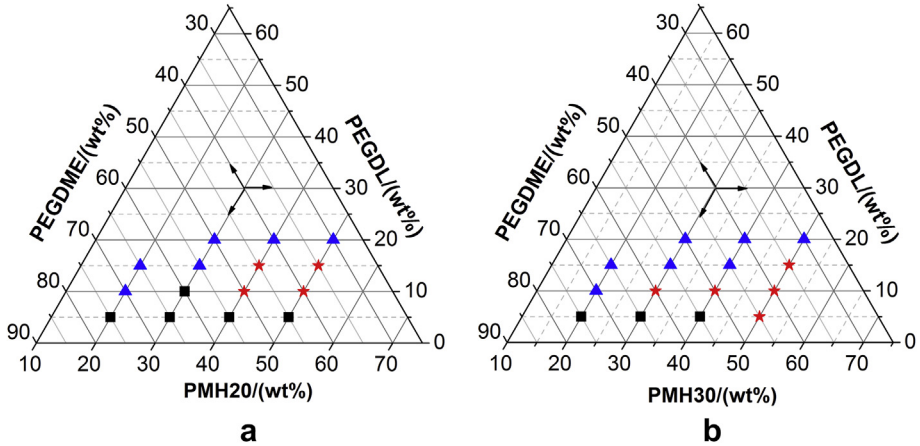

Fig. 3. Dependence of GPE mechanical performance ((★) elastic (■) brittle (▲) plasticizer leakage) on the GPE composition with PMH20, PEGDL and PEGDME (a); PMH30, PEGDL and PEGDME (b).

Table 2
The properties of dimensionally stable electrolytes.

Polymer matrix	Weight ratio (wt%) PMH/PEGDL/PEGDME	σ (10^{-4} S cm^{-1}) at 30 °C	T_g (°C)
PMH20	50/10/40	5.8	–
	50/15/35	4.7	–
	40/10/50	7.3	−69.8
	40/15/45	6.5	−66.7
PMH30	50/5/45	4.9	–
	50/10/40	3.8	–
	50/15/35	3.1	–
	40/10/50	6.1	−65.4
	30/10/60	8.2	−74.3

is composed of 30 wt% PMH30, 10 wt% PEGDL, and 60 wt% PEGDME. Not surprisingly, the bell-shaped conductivity curve versus the lithium salt concentration is observed, which is common for PEO-based electrolytes, since the conductivity is affected by the charge carrier density and the mobility of EO chains. When the lithium salt concentration is low, the salt tends to dissociate to increase the free ion concentration. The number of free ions and the conductivity increase with the lithium salt concentration. However, after the lithium salt concentration reaches certain value, the excess dissociated Li^+ may form ion pairs with ClO_4^-, leading to the decrease the concentration of free ions. In addition, with the increase of the lithium salt concentration, the T_g, which can be attributed to the enhanced inter- and intra-molecular coordination between Li^+ and EO units, further limiting the motion of EO chains and lowering the conductivity [29]. The maximum conductivity, 8.2×10^{-4} S cm^{-1}, is obtained when [Li]:[EO] = 1:20. In the following study, the ratio of [Li]:[EO] is set at 1:20.

3.4. Phase behavior

It is well known that the low T_g is coupled with the high mobility of the EO chains [30]. In order to investigate the effect of the hydrocarbon chains C_{16} from HPEGM and C_{11} chains from PEGDL on the thermal behavior of the GPEs, various solid and gel polymer electrolytes are prepared and studied by DSC. The composition of the studied SPEs and GPEs is listed in Table 3 and Fig. 6 shows the DSC profiles.

In Fig. 6a, the T_g of the samples with partial/all C_{16} end-modification, that is, SPE-2 (−55.3 °C), SPE-3 (−60.1 °C), SPE-4 (−63.3 °C) and SPE-5 (−71.3 °C), is much lower than the T_g of SPE-1 (−47.2 °C), suggesting that C_{16} end-modification improves the mobility of EO chains. In addition, more C_{16} in the SPE polymer matrix leads to lower T_g and higher mobility of EO chains. The possible reasons are as follows: (1) elongated graft chains promotes the flexibility of the main chains; (2) hydrocarbon chains might shield partial Van der Waals force between polar EO chains via the stereo hindrance effect; (3) hydrocarbon chains could reduce the entanglement of the EO chains due to the incompatibility between hydrocarbon and C–O–C groups. The endothermic melting/crystallization peak of hydrocarbon chains [7,31] is only detected in SPE-4 (T_m = −15.2 °C, ΔH_m = 4.3 J g^{-1}) and SPE-5 (T_m = −9.3 °C, ΔH_m = 15.6 J g^{-1}), while no endothermic melting peak of hydrocarbon chains is detected in SPE-2 and SPE-3. It can be inferred that the crystallization temperature of hydrocarbon chains is related to their content in the polymer matrix. More C_{16} chains are easier to crystallize and form physical cross-linking. With certain C_{16} end-capping chains in the polymer matrix, the hydrocarbon chains tend to pack densely due to electrostatic repulsion and become easy to separate from the EO phase.

Fig. 6b shows the DSC traces of different gel electrolytes. After hosting a large amount of plasticizer, GPEs present lower T_g than the corresponding SPEs due to the great free volume expansion of the EO chains by the introduction of plasticizer. The melting enthalpy of hydrocarbon chains in GPEs decreases compared to SPEs because the hydrocarbon phase is diluted by the addition of plasticizer. The same phenomenon that the crystallization temperature of hydrocarbon chains is related to their content is observed in GPEs. When the concentration of C_{16} and C_{11} chains is low, no melting peak is observed in the DSC profiles of both GPE-3-a and GPE-1-a due to sparse packing of hydrocarbon chains in the matrix. When the concentration of C_{16} and C_{11} raises to a higher level as listed in Table 3, the endothermic melting/crystallization peak is detected at −26.7 °C and −46.4 °C in GPE-4 and GPE-1-b, respectively. Due to the difference of the conformational mobility and the degree of freedom between C_{11} and C_{16}, C_{11} chains in GPE-1-b have low melting temperature (−46.4 °C) compared to C_{16} chain in GPE-4 (−26.7 °C) since long hydrocarbon chains are easy to crystallize, which can be used to differentiate the two partially overlapped melting peaks at −42.2 °C of C_{11} and −31.9 °C of C_{16} in the DSC trace of GPE-3-b. The overlapping of melting peaks is probably caused by the C_{16}/C_{11} mixed phase. While the phase of EO chains is amorphous at the temperature range of the test, the hydrocarbon chains and EO chains of the electrolyte seem to be strongly segregated below the melting point (T_m) of the hydrocarbon chains [32]. At room temperature, the sample of GPE-3-b looks slightly hazy, indicating the possible phase separation [19,32]. With the addition of PEGDL to replace 10 wt% PEGDME, the T_g increases to −74.3 °C (GPE-3-b) from −81.1 °C (GPE-3-a). Although both PEGDME and PEGDL act as the plasticizer to promote the mobility of EO chains and reduce the T_g, PEGDL has another function as the physical cross-linking agent. Due to the formation of physical cross-linking, PEGDL slightly limits the mobility improvement of EO chains compared to PEGDME. In contrast to GPE-3-a and GPE-3-b, GPE-6 is prepared by using PEGDA to form chemical cross-linking. The T_g of GPE-6 (−72.7 °C) is higher than that of GPE-3-a and GPE-3-b, since the chemical cross-linking greatly restrains the motion of polymer chains.

3.5. Thermal stability

The thermal stability of electrolytes is analyzed by thermogravimetry under N_2 atmosphere as shown in Fig. 7. In the temperature range from 80 °C to 195 °C, no mass loss is observed in SPE-3, while GPE-3-a and GPE-3-b show small amount of weight loss, 4.9% and 2.8%, respectively, presumably caused by the evaporation of low molecular weight components in the PEGDME [27]. In the temperature range from 195 °C to 270 °C, the weight loss of GPE-3-a and GPE-3-b is 43.4% and 34.1%, respectively, which may correspond to the evaporation of major ingredient in PEGDME. After the temperature exceeds 270 °C, the C–O–C groups in the polymer electrolytes begin to pyrolyze [20,29,33]. The rate of pyrolysis increases rapidly with temperature, especially in SPE-3. The presence of PEGDME and PEGDL in the polymer matrix does not alter the pyrolysis temperature of the C–O–C groups.

3.6. Mechanical property

Fig. 8a and b shows the stress–strain curves of SPE and GPE films, respectively. The results reveal the dependence of the film mechanical property on the composition. With the increase of HPEGM content or physical cross-linking density, the SPE films appear from brittle to ductile, while the SPE-6 film is stiff and brittle due to chemical cross-linking. The physically cross-linked SPE films show larger elongation than the chemical cross-linked SPE-6. The same phenomenon is observed in GPE films. The presence of hydrocarbon chains enhances both the stress and strain behavior of

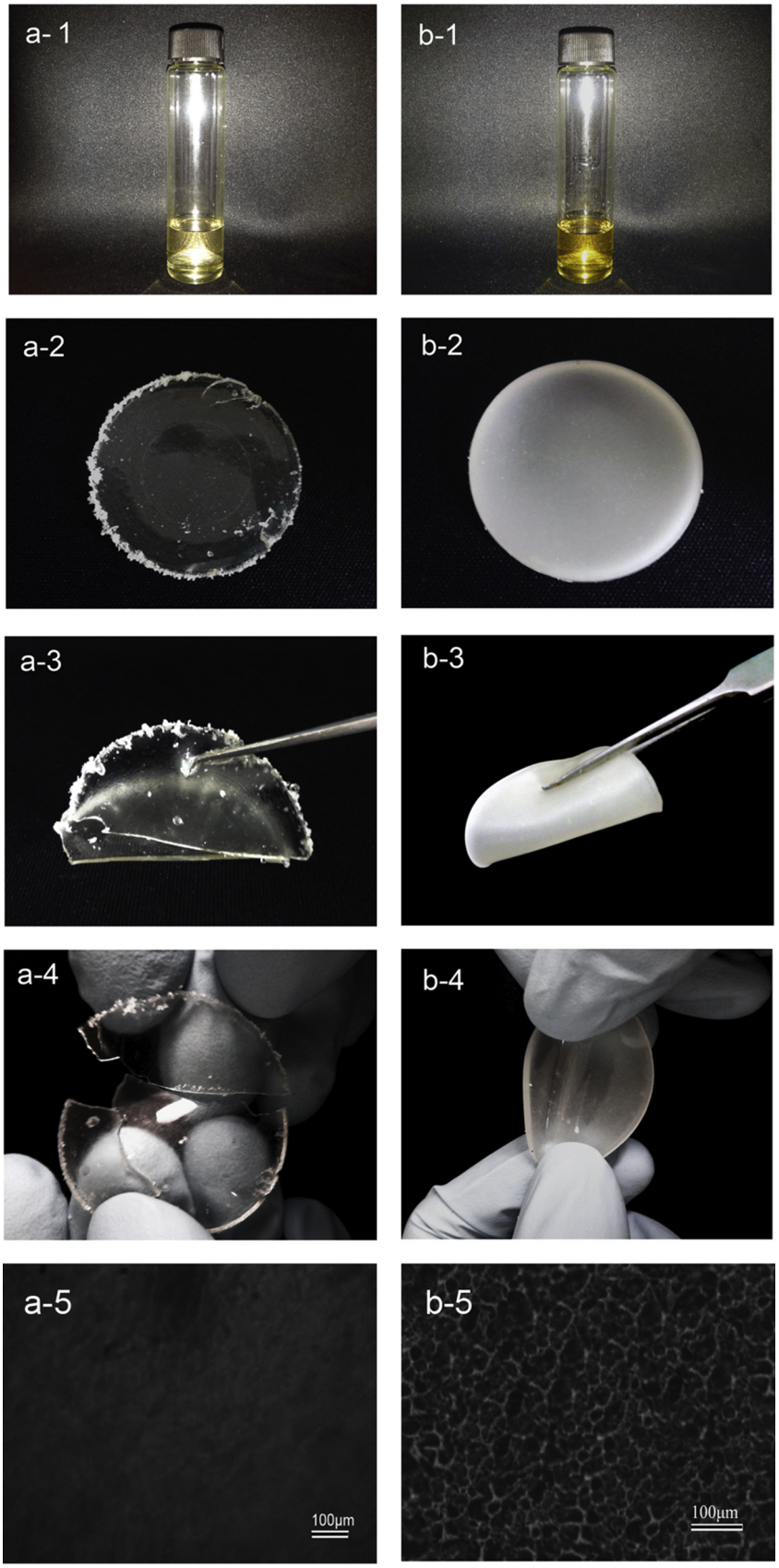

Fig. 4. Visualized mechanical difference with/without PEGDL. The photographs of the reaction mixtures (1); the photographs of the GPE films (2); the results of preliminary mechanical test: bending test (3) and tensible test (4); the microscopic appearance of GPE films (5); PMH30:PEGDME = 30:70 (wt%) without PEGDL (a); PMH30:PEGDL:PEGDME = 30:10:60 (wt%) (b).

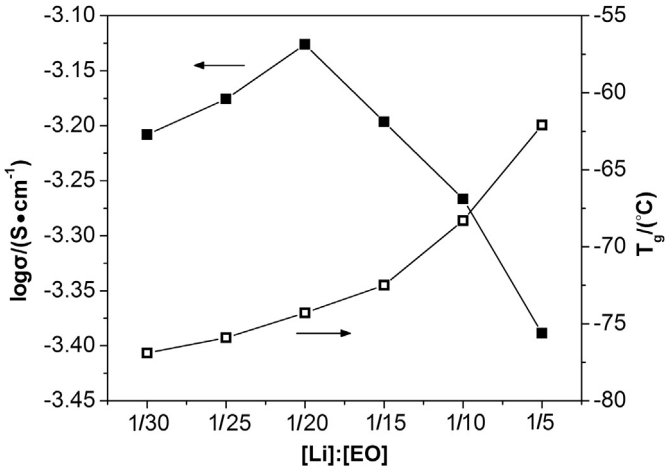

Fig. 5. The dependence of the ionic conductivity and T_g on the concentration of lithium salt while GPE composition is 30 wt% PMH70, 10 wt% PEGDL and 60 wt% PEGDME.

the electrolyte films, that is beneficial to the lithiation/delithiation process since the process normally involves volume change of the electrodes. A stiff and brittle electrolyte film can lead to incomplete contact with the electrode, that is detrimental to electrochemical performance. The GPE films with the stress between 0.38 MPa and 0.52 MPa at an elongation-at-break value (strain) up to 10% are of good mechanical strength.

3.7. Transference number measurement

The bulk and interfacial resistance of the Li/polymer electrolyte/Li cell before and after polarization is measured by AC impedance and plotted in Fig. 9. The inserted figure is the depolarization curve of the cell when the sample is subject to a small dc polarization potential (50 mV) for sufficient time to reach steady-state. Table 4 summarizes the data related to the t_+ calculation for SPE-3, GPE-2, GPE-3-a and GPE-3-b. The transference number of the solid polymer electrolyte (SPE-3) is similar to that of the gel polymer electrolytes, suggesting that the anion contributes to the total ionic conductivity much more than cation in both SPE and GPE.

3.8. Ionic conductivity

Fig. 10 plots the dependence of log σ on $1/T$ in the temperature range between 10 °C and 80 °C for SPE-3, GPE-3-a, GPE-3-b and GPE-6. The curves show slightly positive deviation from the

Table 3
The composition of the polymer electrolytes at [Li]:[EO] = 1:20.

Polymer electrolytes	Component	Weight ratio of the components (wt%)
SPE-1	PMPEGM	100
SPE-2	PMH20	100
SPE-3	PMH30	100
SPE-4	PMH50	100
SPE-5	PHPEGM	100
SPE-6	PMH30/PEGDA[a]	85/15
GPE-1-a	PMPEGM/PEGDL/PEGDME	30/10/60
GPE-1-b	PMPEGM/PEGDL/PEGDME	30/20/50
GPE-2	PMH20/PEGDL/PEGDME	40/10/50
GPE-3-a	PMH30/PEGDME	30/70
GPE-3-b	PMH30/PEGDL/PEGDME	30/10/60
GPE-4	PMH50/PEGDME	50/50
GPE-6	PMH30/PEGDA/PEGDME	25.5/4.5/70

[a] Chemical cross-linker: poly(ethylene glycol) diacrylate (PEGDA575, aladdin).

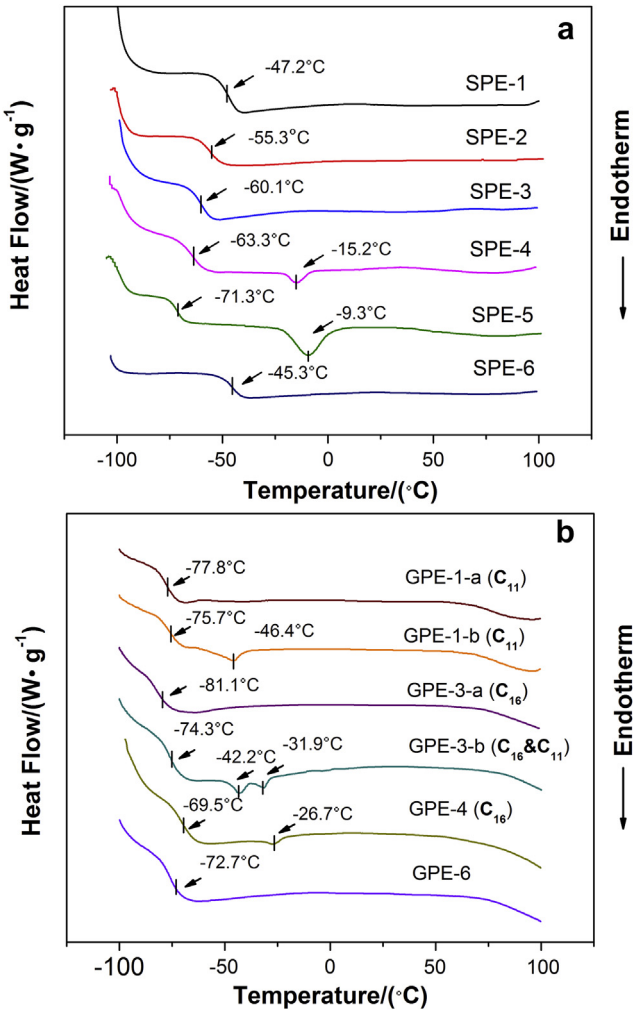

Fig. 6. DSC traces for polymer electrolytes, (a) solid polymer electrolytes, (b) gel polymer electrolytes.

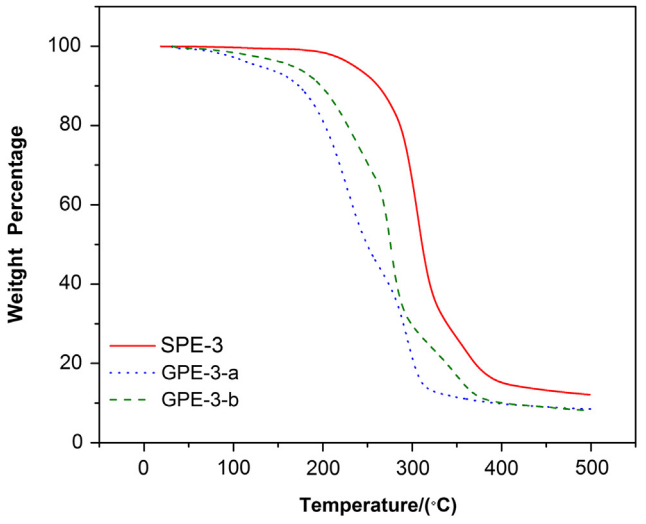

Fig. 7. TG profiles for polymer electrolytes.

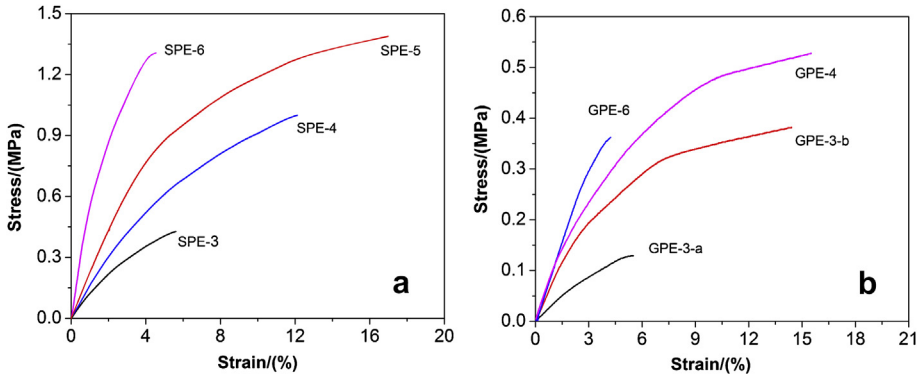

Fig. 8. Stress–strain plots for polymer electrolytes, (a) solid polymer electrolytes, (b) gel polymer electrolytes.

Arrhenius relationship, which can be classified as a type of Vogel–Tamman–Fulcher (VTF) model as the following:

$$\sigma = AT^{-1/2}\exp^{-E_a/R(T-T_0)} \quad (3)$$

where A is the constant proportional to the number of carrier ions, E_0 is the pseudo-activation energy related to the motion of the polymer segment, R is the Boltzmann constant, and T_0 is the reference temperature, normally associated with the ideal T_g at which the free volume is zero or with the temperature at which the configuration entropy becomes zero [34]. The VTF expression implies that the ion conduction in polymer electrolytes is affected by the segmental motion of the EO chains [15,17,35,36]. According to the Adam–Gibbs analysis, T_0 is usually taken as 50 K below the measured T_g. The fitted parameter, A, E_0, and T_0 are listed in Table 5. The solid polymer electrolyte SPE-3 has a high E_0 value (8.4 kJ mol^{-1}) compared to the gel polymer electrolytes (5.6–6.4 kJ mol^{-1}). The chemical cross-linked polymer electrolyte GPE-6 exhibits a higher E_0 and a lower conductivity (6.5×10^{-4} S cm^{-1} at 30 °C) than the physically cross-linked GPE-3-b. The reason is that the mobility of the polymer chains is greatly hindered by the chemical covalent bond produced by chemical cross-linker PEGDA. Thus, the introduction of plasticizer in GPEs encourages the motion of EO chains, lowers the required activation energy, decreases the glass transition temperature and improves the lithium ion conductivity in the polymer electrolytes.

3.9. Electrochemical stability of gel electrolyte GPE-3-b

In order to study the electrochemical stability of GPE-3-b, cyclic voltammogram was performed with Pt as the working electrode and Li as the reference and counter electrode, and plotted in Fig. 11. The oxidation peak appears at 4.5 V vs. Li$^+$/Li, while the reversible lithium plating/stripping takes place in the potential range of −0.5 V to 0.5 V (vs. Li$^+$/Li). Therefore, the obtained polymer electrolyte has stable potential window up to 4.5 V as well as reversible plating/stripping of Li on the Pt electrode, which could be applied to the practical lithium polymer cell [15].

3.10. Interface stability between lithium electrode and GPE-3-b

The interfacial stability between electrolyte and electrode is a key factor since uncontrolled passivation on the lithium electrode may cause serious safety issues. The commercial PEGDME contains trace amount of residual hydroxyl groups which may increase the interfacial resistance between lithium electrode and electrolyte.

Table 4
The data related to Li$^+$ transference number of electrolytes at [Li]:[EO] = 1:20.

Electrolyte	$R_{b,0}$ (Ω)	$R_{b,s}$ (Ω)	$R_{i,0}$ (Ω)	$R_{i,S}$ (Ω)	I_0 (mA)	I_s (mA)	t_+
SPE-3	233.7	238.5	685.2	873.4	0.051	0.026	0.28
GPE-2	17.2	19.4	68.8	132.4	0.568	0.228	0.25
GPE-3-a	22.5	26.2	70.7	129.3	0.528	0.211	0.26
GPE-3-b	15.6	17.5	53.1	107.1	0.716	0.265	0.23

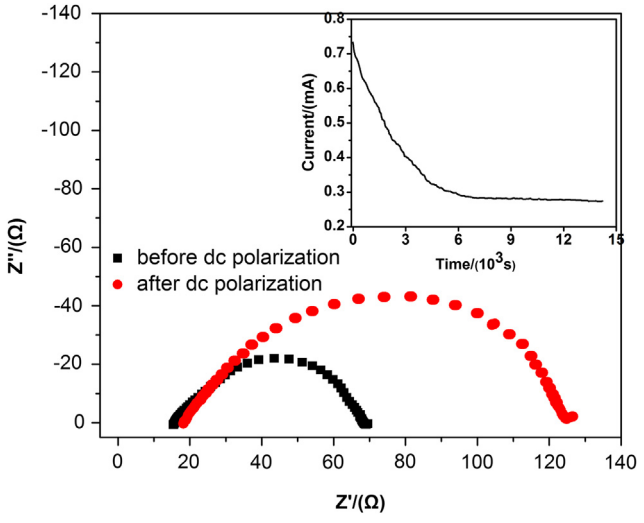

Fig. 9. Impedance spectra of the Li/GPE-3-b/Li cell measured before and after polarization at 30 °C. Inserted figure: depolarization curve of the cell.

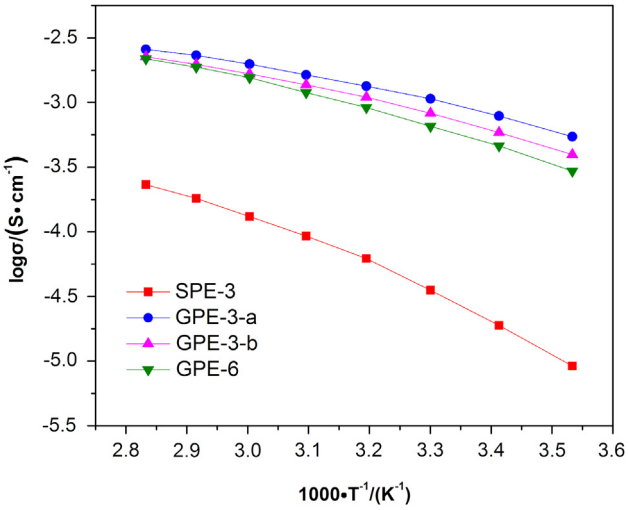

Fig. 10. Temperature dependence of ion conductivity of polymer electrolytes.

Table 5
VTF fitted parameters for electrolytes at [Li]:[EO] = 1:20.

Sample	A (S $K^{1/2}$ cm^{-1})	E_0 (kJ mol^{-1})	T_0 (K)	T_g (K)
SPE-3	0.9	8.4	162.7	212.7
GPE-3-a	1.2	5.6	141.9	191.9
GPE-3-b	1.3	5.7	148.7	198.7
GPE-6	1.9	6.4	152.4	202.4

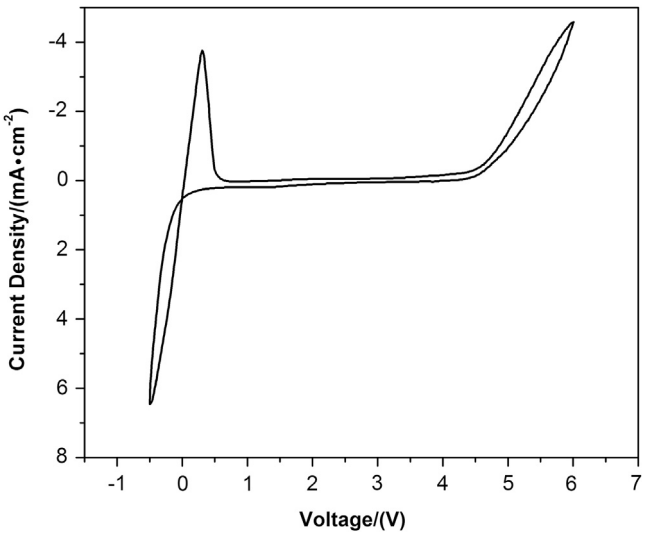

Fig. 11. The cyclic voltammograms of Pt/GPE-3-b/Li cell swept from −0.5 V to 6.0 V vs. Li^+/Li at 30 °C, the scan rate is 5 mV s^{-1}.

Here the detriment of the residual hydroxyl groups is explored through the interface stability by comparing pretreated and untreated PEGDME in GPEs.

The interface stability between the lithium and the gel electrolytes is evaluated by measuring the AC impedance of Li/GPE-3-b/Li cell stored at 30 °C under open-circuit potential condition. Fig. 12a presents the change of the impedance spectra of the cell containing the pretreated PEGDME with time. It can be seen clearly that the bulk resistance (R_b) changes little during the storage and stabilizes at around 10 Ω, suggesting that GPE-3-b with treated PEGDME can maintain composition constant. The interface resistance (R_i) shows a progressive increase to a steady value at about 115 Ω after 15 days. R_i comes from the resistance of the passivation film formed on the lithium electrode and the charge-transfer resistance. The R_i increase is mainly attributed to the formation of a passivation film on the surface of the lithium electrode due to residual impurities in the gel electrolyte.

Fig. 12b shows the change of the impedance spectra of the cell containing the untreated PEGDME with time. With the existence of the trace amount of residual hydroxyl groups, the gel electrolyte presents completely different interface stability. The R_i jumps to about 400 Ω after 40 days. In addition, R_b has slight increase during the storage. The change of R_i and R_b indicates that the composition of the gel polymer electrolyte is altered by the possible reaction between hydroxyl groups and lithium electrode.

The above impedance results imply that PEGDME pretreatment makes GPE more compatible with the lithium electrode. Therefore the PEGDME has to be treated to eliminate the residual hydroxyl groups before use as the plasticizer.

3.11. Cell testing

The charge–discharge profiles of the Li/GPE-3-b/$LiFePO_4$ 2032 coin-type cell at different C-rate are shown in Fig. 13a (at 30 °C) and Fig. 13b (at 50 °C). When the cell is cycled at 30 °C, the discharge capacities are 152, 130, 89, and 54 mAh g^{-1}, at 0.1 C, 0.2 C, 0.5 C, and 1 C, respectively. To our best knowledge, 152 mAh g^{-1} at 0.1 C is the highest discharge capacity reported so far in $LiFePO_4$/PEGDME based gel polymer electrolytes/Li systems. The discharge capacity improvement may be ascribed to the relatively high conductivity of the GPE-3-b electrolyte and elimination of the hydroxyl groups in PEGDME which avoid the side reaction between electrolyte and metallic lithium. The dramatically decrease of the discharge capacity with the increase of the C-rate may be attributed to the slow Li^+ diffusion within the $LiFePO_4$ electrode which is not moistured by electrolyte, the relatively low ionic conductivity of the polymer electrolyte compared to liquid electrolyte, and the formation of a barrier potential due to the anion accumulation in the vicinity of the anode–electrolyte interface which further hinders the motion of Li^+ during discharge [37,38]. When the cell is cycled at 50 °C, the discharge capacities are 163, 146, 125, and 107 mAh g^{-1}, at 0.1 C, 0.2 C, 0.5 C, and 1 C, respectively. The great charge–discharge performance improvement of the Li/GPE-3-b/$LiFePO_4$ cell at 50 °C suggests that both transport and reaction kinetics are enhanced at elevated temperatures.

In Fig. 14, long term cycling behaviors of the Li/GPE-3-b/$LiFePO_4$ 2032 coin-type cell at 0.1 C and 0.2 C are investigated at different temperatures. The discharge capacity remains 88.2% of its initial discharge capacity after 50 cycles at 0.1 C at 30 °C. In addition, the coulombic efficiency is still more than 95% at the 50th cycle. The good cycling stability at a low current can be attributed to the

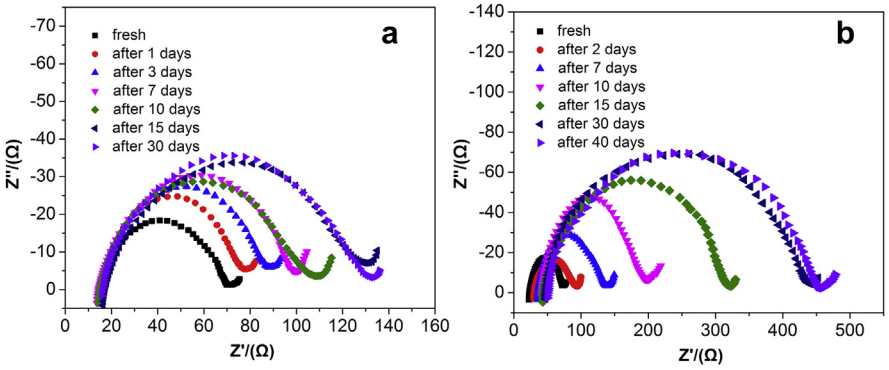

Fig. 12. Impedance spectra of Li/GPE-3-b/Li cell: (a) with pretreated PEGDME, (b) with untreated PEGDME.

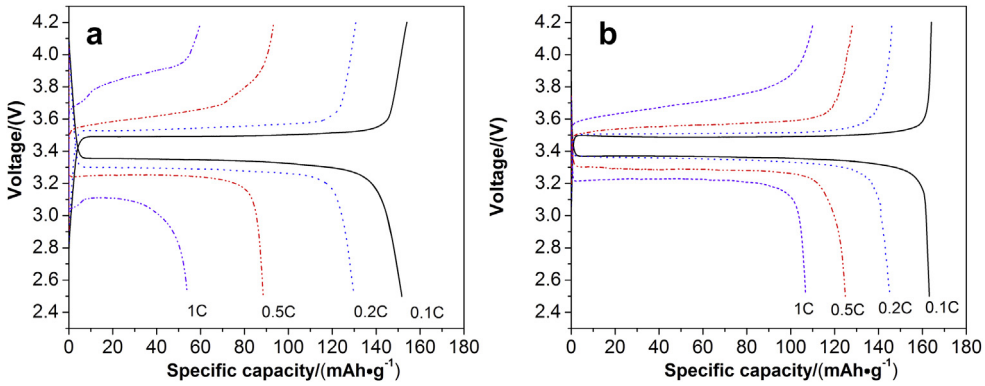

Fig. 13. Charge–discharge curves of Li/GPE-3-b/$LiFePO_4$ cell at different rates at 30 °C (a) and 50 °C (b).

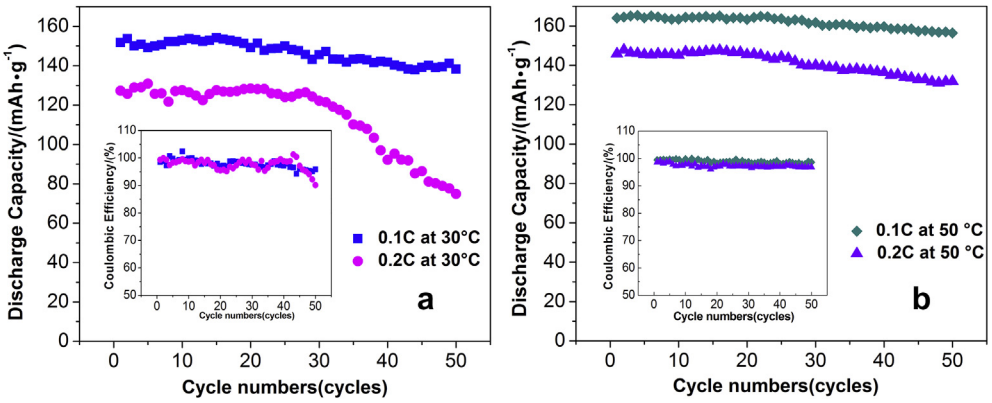

Fig. 14. Cycle life test of Li/GPE-3-b/$LiFeO_4$ cell at 0.1 C and 0.2 C. Inserted figure: coulombic efficiency vs cycle number at different rates. At (a) 30 °C, (b) 50 °C.

relatively good interfacial contact between electrodes and GPE-3-b film. However, the good contact may lose when the electrode presents a quick thickness change during lithiating/delithiating at 0.2 C under 30 °C. Therefore, the repeated local strip and adhesion in atomic scale between the polymer electrolyte and the electrodes, cause the fluctuation coulombic efficiency throughout the cycling. The GPE film gradually strips from the electrodes after 27 cycles, which leads to a continuous fading of the discharge capacity [39]. However, the high coulombic efficiency, over 98%, may due to that the stable SEI film is formed completely during the formation cycles. The introduction of a more flexible polymer with a better adhesion property may improve the high-rate cycling performance. When the cell is cycled at 50 °C, since the GPE film exhibits better adhesion at a high temperature, the repeated local strip and adhesion in atomic scale between the polymer electrolyte and the electrodes may not occur. Therefore, the capacity retention of Li/GPE/$LiFePO_4$ cell is quite stable. After 50 cycles, the discharge capacity of the Li/GPE-3-b/$LiFePO_4$ cell remains 95.3% and 90.4% of its initial discharge capacity, respectively.

4. Conclusion

The incorporation of PEGDL, a new physical cross-linking agent/secondary plasticizer, into the gel polymer electrolyte does enhance the mechanical property and ensure the conductivity. The gel polymer electrolyte composed of 30 wt% PMH30, 10 wt% PEGDL, and 60 wt% PEGDME, is labeled as GPE-3-b in this study. GPE-3-b presents good mechanical properties due to the formation of physical cross-linking between C_{16} chains in PMH30 and C_{11} chains in PEGDL, and exhibits a relatively high conductivity (8.2×10^{-3} S cm^{-1} at 30 °C) at the optimum $LiClO_4$ concentration ([Li]:[EO] = 1:20). In addition, GPE-3-b shows an excellent interfacial stability with metallic lithium after the elimination of the residual hydroxyl groups in PEGDME. Then a coin cell based on GPE-3-b, with $LiFePO_4$/C as cathode and metallic lithium as anode, shows discharge capacity as high as 152 mAh g^{-1} and 163 mAh g^{-1} when cycled at 30 °C and 50 °C under a current density of 0.1 C, respectively.

Acknowledgements

This work was supported by Key Project of Natural Science Foundation of Jiangsu Province of China (gs1) (Grant No. BK2011030), Key Project of Educational Commission of Jiangsu Province of China (gs2) (Grant No. 11KJA430006) and the Priority Academic Program Development of Jiangsu Higher Education Institutions.

Supplementary data

Supplementary data related to this article can be found at http://dx.doi.org/10.1016/j.jpowsour.2013.03.144.

References

[1] M. Armand, J.M. Tarascon, Nature 451 (2008) 652–657.
[2] H.J. Ha, E.H. Kil, Y.H. Kwon, J.Y. Kim, C.K. Lee, S.Y. Lee, Energy Environ. Sci. 5 (2012) 6491–6499.
[3] D.E. Fenton, J.M. Parker, P.V. Wright, Polymer 14 (1973) 589.
[4] P. Judeinstein, F. Roussel, Adv. Mater. 17 (2005) 723–727.
[5] W.H. Meyer, Adv. Mater. 10 (1998) 439–448.

[6] E. Quartarone, P. Mustarelli, Chem. Soc. Rev. 40 (2011) 2525–2540.
[7] P. Jannasch, Macromolecules 33 (2000) 8604–8610.
[8] H.R. Allcock, S.J.M. O'Connor, D.L. Olmeijer, M.E. Napierala, C.G. Cameron, Macromolecules 29 (1996) 7544–7552.
[9] Z.C. Zhang, D. Sherlock, R. West, R. West, Macromolecules 36 (2003) 9176–9180.
[10] R. Hooper, Macromolecules 34 (2001) 931–936.
[11] J.F. Snyder, R.H. Carter, E.D. Wetzel, Chem. Mater. 19 (2007) 3793–3801.
[12] A.M. Elmér, P. Jannasch, Solid State Ionics 177 (2006) 573–579.
[13] M. Andrei, M. Soprani, Polymer 39 (1998) 7041–7047.
[14] S. Tobishima, H. Morimoto, M. Aoki, Y. Saito, T. Inose, T. Fukumoto, T. Kuryu, Electrochim. Acta 49 (2004) 979–987.
[15] Y. Kang, H.J. Kim, E. Kim, B. Oh, J.H. Cho, J. Power Sources 92 (2001) 255–259.
[16] J.H. Shin, S.S. Jung, K.W. Kim, H.J. Ahn, J. Mater. Sci-Mater. El. 12 (2002) 727–733.
[17] Y. Kang, J. Lee, D.H. Suh, C. Lee, J. Power Sources 146 (2005) 391–396.
[18] J.J. Xu, H. Ye, Electrochem. Commun. 7 (2005) 829–835.
[19] Y. Kang, J. Lee, J. Lee, C. Lee, J. Power Sources 165 (2007) 92–96.
[20] M. Ueno, N. Imanishi, K. Hanai, T. Kobayashi, A. Hirano, O. Yamamoto, Y. Takeda, J. Power Sources 196 (2011) 4756–4761.
[21] G. Liu, G.L. Baker, Soft Matter 4 (2008) 1094–1101.
[22] G. Liu, M. Reinhout, B. Mainguy, G.L. Baker, Macromolecules 39 (2006) 4726–4734.
[23] X. Zuo, X.M. Liu, F. Cai, H. Yang, X.D. Shen, G. Liu, J. Mater. Chem. 22 (2012) 22,265–22,271.
[24] V.I. Raman, G.R. Palmese, Langmuir 21 (2005) 1539–1546.
[25] J. Lee, G.R. Yandek, T. Kyu, Polymer 46 (2005) 12511–12522.
[26] J. Evans, C.A. Vincent, P.G. Bruce, Polymer 28 (1987) 2324–2328.
[27] K.M. Abraham, Z. Jiang, B. Carroll, Chem. Mater. 9 (1997) 1978–1988.
[28] T. Niitani, M. Shimada, K. Kawamura, K. Kanamura, J. Power Sources 146 (2005) 386–390.
[29] Y.H. Liang, C.C. Wang, C.Y. Chen, Eur. Polym. J. 44 (2008) 2376–2384.
[30] Y. Masuda, M. Seki, M. Nakayama, M. Wakihara, H. Mita, Solid State Ionics 177 (2006) 843–846.
[31] P. Jannasch, Electrochim. Acta 46 (2001) 1641–1649.
[32] P. Jannasch, Polymer 41 (2000) 6701–6707.
[33] S.M. Lee, W.L. Yeh, C.C. Wang, C.Y. Chen, Electrochim. Acta 49 (2004) 2667–2673.
[34] K.M. Abraham, M. Alamgir, J. Electrochim. Soc. 137 (1990) 1657–1658.
[35] P. Jannasch, Chem. Mater. 14 (2002) 2718–2724.
[36] M.H. Ryou, Y.M. Lee, K.Y. Cho, G.B. Han, J.N. Lee, D.J. Lee, J.W. Choi, J.K. Park, Electrochim. Acta 60 (2012) 23–30.
[37] S. Tan, S. Walus, J. Hilborn, T. Gustafsson, D. Brandell, Electrochem. Commun. 12 (2010) 1498–1500.
[38] C. Gerbaldi, Ionics 16 (2010) 777–786.
[39] M. Wang, S. Dong, J. Power Sources 170 (2007) 425–432.